

Quasiparticle Dispersion of the 2D Hubbard Model: From an Insulator to a Metal

R. Preuss and W. Hanke

*Institut für Theoretische Physik, Universität Würzburg, Am Hubland
D-97074 Würzburg, Germany*

W. von der Linden

*Max-Planck-Institut für Plasmaphysik, EURATOM Association
D-85740 Garching b. München, Germany*

(May 15, 2018)

Abstract

On the basis of Quantum-Monte-Carlo results the evolution of the spectral weight $A(\vec{k}, \omega)$ of the two-dimensional Hubbard model is studied from insulating to metallic behavior. As observed in recent photoemission experiments for cuprates, the electronic excitations display essentially doping-independent features: a quasiparticle-like dispersive narrow band of width of the order of the exchange interaction J and a broad valence- and conduction-band background. The continuous evolution is traced back to one and the same many-body origin: the doping-dependent antiferromagnetic spin-spin correlation.

PACS numbers: 71.30.+h, 74.72.-h, 79.60.-i

Recent results of angle resolved photoemission spectroscopy (“ARPES”) [1] revealed strong similarities in the low-energy excitations of a proto-type insulating copper oxide, i.e. $Sr_2CuO_2Cl_2$ [2], and metallic cuprates like $Bi\ 2212$, $Bi\ 2201$, etc.: in both cases the quasiparticle (QP) band has rather small dispersion of typically 1 eV width, it is separated from a broad main valence-band “background” (of about 6 eV width) in much the same way, the \vec{k} -dispersion is similar and also the intensity modulation as function of energy is comparable. Thus, it appears that the dispersive metallic band evolves continuously from the insulating limit and has a similar physical origin as the undoped valence band in the cuprates. This has important consequences for the copper oxides: the excitation spectrum in the insulating case is decisively determined by many-body effects, documented by the known difficulties of one-electron bandstructure calculations for the insulating limit [1], which then strongly emphasizes a many-body origin of the QP dispersion also in the metallic case.

In this work Quantum-Monte-Carlo (QMC) results for the angular resolved photoemission spectral weight $A(\vec{k}, \omega)$ for the two-dimensional (2-D) Hubbard model are reported which demonstrate for this “generic” model the above strong similarities between undoped insulating and doped metallic situations: in particular, we find in both cases a very similar small dispersive low-energy band, for which the band width is set by the exchange interaction $J \sim 4t^2/U$ when the Coulomb correlation U is of order of the non-interacting bandwidth $8t$. This new feature is shown in the metallic case to be essentially unrenormalized (for electronically filled, i.e. $\omega < \mu$ states) from the insulating band, while above the chemical potential μ additional states with again an energy scale set by J are filled in. $A(\vec{k}, \omega)$ is inferred from the QMC data by applying Bayesian probability theory in the frame of “quantified maximum entropy” [3,4]. A consistent treatment of hyper-parameters and error-covariances along with high-quality QMC-data allows to reveal details of the low-lying excitations which have not been seen before in QMC simulations. On the basis of these QMC results and the strong similarities to ARPES data in both insulators and metals, we argue that the continuous evolution of the QP dispersion relation observed in the high- T_c cuprates arises from a common many-body origin, namely from the continuous change of the spin-spin correlation length ξ

and the related changes in the hole-spin correlations [5]. Similarities to a phenomenology by Kampf and Schrieffer [6], where the magnetic correlation length ξ is an input parameter, are pointed out.

In the insulating and metallic case, respectively, the QP-like band is separated similarly from a broad “incoherent” background, extending about $6t$ to $8t$. The latter corresponds to upper and lower Hubbard bands and follows in intensity and energy spread roughly the weak-coupling spin-density-wave (SDW) prediction, as already reported in earlier QMC simulations by Bulut, Scalapino and White [7–9].

Our results confirm, but also extend these simulation results: As stated in this previous work the available resolution was such that when \vec{k} moved below the Fermi surface only the $6t$ to $8t$ broad lower Hubbard band could be resolved both for the insulating [7] and the metallic [8] cases. However, it was already suspected there that a narrow QP band exists, since such a band of width J has been found for one-hole doped in an AF insulating t-J model [10,11]. Narrow QP bands were also observed for finite dopings in exact-diagonalization calculations of the one-band Hubbard [12–15] and t-J [16] models, as well as in QMC-results for the three-band Hubbard model [17].

The single-band 2-D Hubbard model has the Hamiltonian

$$H = -t \sum_{\langle i,j \rangle, \sigma} (c_{i,\sigma}^\dagger c_{j,\sigma} + h.c.) + U \sum_i n_{i\uparrow} n_{i\downarrow} \quad (1)$$

on a square lattice, where t is the near-neighbor hopping, $c_{i,\sigma}$ destroys an electron of spin σ on site i and $n_{i,\sigma} = c_{i,\sigma}^\dagger c_{i,\sigma}$. The chemical potential μ sets the filling $\langle n \rangle = \langle n_{i,\uparrow} + n_{i,\downarrow} \rangle$. Here we focus on results obtained both for half-filling $\langle n \rangle = 1$ and other fillings in order to develop a systematic picture of the low-lying electronic excitations as a function of doping. The Coulomb correlation U is chosen equal to the bandwidth $8t$ and as $U = 12t$.

In order to obtain from the QMC data for the single-particle finite-temperature propagator $G(\vec{k}, \tau)$ the corresponding spectral weight $A(\vec{k}, \omega)$ for real frequencies ω , the following Laplace transform has to be inverted:

$$G(\vec{k}, \tau) = - \int_{-\infty}^{\infty} A(\vec{k}, \omega) \frac{e^{-\tau\omega}}{1 + e^{-\beta\omega}} d\omega \quad (2)$$

It is by now well established [18–22] that the maximum-entropy method [3,4] provides a controlled way to infer the most reliable $A(\vec{k}, \omega)$ in the light of the QMC data. To achieve the desired resolution, it is important to use a likelihood function which takes the error-covariance matrix of the QMC data and its statistical inaccuracy consistently into account [23]. The results presented in this letter are based on QMC data with good statistics, i.e. averages over 10^5 updates of all the Hubbard-Stratanovich variables result in $G(\vec{k}, \tau)$'s with statistical error less than 0.5%. Correlations of the data in imaginary time were considered by making use of the covariance matrix in the MaxEnt-procedure [24]. As suggested in previous work by White [19], various moments of the spectral weight were also incorporated in extracting $A(\vec{k}, \omega)$. In order to check on this analytical-continuation procedure detailed comparisons with 4×4 exact diagonalizations [13–15] have been performed.

The results presented here are for lattices 8×8 in size and for temperatures ranging from $\beta t = 3$ ($T = 0.33t$) to $\beta t = 10$ ($T = 0.1t$). Covering this temperature range allows us in effect to study (at half-filling) a situation where the spin-spin correlation length ξ is larger (for $\beta t = 10$) than the lattice size. In this case the system behaves as if it were at $T = 0$ and develops an AF gap. For $\beta t = 3$, on the other hand, the spin-spin correlation length is shorter than our finite lattice and, consequently, the gap is diminished and metallic fluctuations exist [20]. As we will see, the latter situation is especially useful in interpreting the QMC data in the metallic (doped) regime and to relate them to those of the insulating (half-filled) case.

We start in Fig. 1 by examining the single-particle spectral weight for $U = 8t$, $\beta t = 10$, at half-filling, i.e. $\langle n \rangle = 1$. Fig. 1(a) gives a 3-D plot of $A(\vec{k}, \omega)$ versus ω for \vec{k} -values out of the Brillouin zone, whereas Fig. 1(b) summarizes these results in the usual “bandstructure” ω versus \vec{k} plot. Here dark (white) areas correspond to a large (small) spectral weight.

We observe in all spectra (also in the $U = 12t$, half-filled case, presented in Fig. 3) two general features: One is that $A(\vec{k}, \omega)$ contains a rather dispersion-less “incoherent background”, extending both for electronically occupied ($\omega < \mu$) states and unoccupied ($\omega > \mu$) states over $\sim 6t$ ($\sim 6 eV$) in the $U = 8t$ case. The new structure, which was not previously

resolved in QMC work is a dispersing structure at low energies with small width of the order of J , which defines the gap Δ and which, (at least for $U = 12t$), is well separated from the higher energy background.

The splitting in the low-energy “band” and the higher-energy “background” is especially pronounced near Γ -(for $\omega < \mu$) and M-(for $\omega > \mu$) points due to a relative weight shift from negative to positive energies as \vec{k} moves through X or equally through $(\pi/2, \pi/2)$, the midpoint between Γ and M. The overall weight distribution in $A(\vec{k}, \omega)$ follows roughly the SDW prediction as found in the QMC calculation by Bulut et al. [7]: the total integrated weight in the SDW approximation $\langle n_{\vec{k}}^{SDW} \rangle = \int_{-\infty}^0 A^{SDW}(\vec{k}, \omega) d\omega$, is in good accord with the QMC momentum distribution [7].

However, the dispersion of the structure near the gap does not follow the SDW prediction: its dispersion has a significant (about a factor of 2 for $U = 8t$) smaller width set by the value of J . This result is in good accord with the dispersion and width found for the low energy “foot” in recent angle-resolved photoemission (ARPES) data [2] and t-J model results (there $t \approx 0.4 eV$) [10]. This is illustrated in Fig. 1(b), where the low-energy peaks in $A(\vec{k}, \omega)$ are fitted by (full and dotted lines) $E_{\vec{k}} = \Delta + J/2(\cos k_x + \cos k_y)^2$, with $\Delta = 2.4t$, rather than by the SDW (strong-coupling) result, i.e. $E_{\vec{k}} = \sqrt{\epsilon_k^2 + \Delta^2} \cong \Delta + J(\cos k_x + \cos k_y)^2$. The overall agreement between the ARPES width and the Hubbard model data (for $t \approx 1eV$) is significant because it shows in fact that the energy scale of the low-lying insulating band is controlled by many-body effects beyond the mean-field SDW result.

Our findings for the spectral-weight dispersion $\omega(\vec{k})$ are schematically summarized in Fig. 2(a), which emphasizes again the different energy scales (J , U , SDW [25]) involved. These energy scales become particularly pronounced in the ($U = 12t$)-case in Fig. 3.

Before moving to the doped situation, we note that the $\beta t = 3$, $U = 12t$ result in Fig. 3 does have the valence-band maximum at the M-point and not at the X- or $(\pi/2, \pi/2)$ -points in contrast to the $\beta t = 10$ results for both $U = 8t$ and $U = 12t$ (not shown). This at first puzzling “high-temperature” result reflects the fact that at $\beta t = 3$ the spin-spin correlation length ξ is about a factor of 2.5 smaller than the QMC lattice extension. The system then

shows precursor effects of a metal, which move the spectral weight (valence-band) maximum – in agreement with the metallic situation in Fig. 4 – to the M-point. Otherwise, the low-energy band is found to be essentially unaffected by changing temperature from $T = 0.1t$ to $T = 0.33t$.

Keeping this in mind, we consider in Fig. 4 the low-energy electronic structure in the metallic regime for doping $\langle n \rangle = 0.95$. 4(a) shows again the 3-D plot of $A(\vec{k}, \omega)$ and 4(b) the dispersion relation with the degree of shading representing the intensity of $A(\vec{k}, \omega)$, as in Fig. 1(b). Like in the half-filled case, we observe two general features, which are both seen in recent photoemission experiments [1]: a broad “background” of $\approx 4t - 6t$ spanning the lower and upper Hubbard band and a pronounced low-energy “foot” of significantly smaller width, which is clearly resolved between $\Gamma \rightarrow X$ and $\Gamma \rightarrow (\pi/2, \pi/2)$. The situation is depicted schematically in Fig.2b. Width and dispersion of the low-energy “band” are also in good accord with exact diagonalization results of 4×4 clusters [13,15].

The results for the doped case have several important implications: First, they reveal that the lowest energy “band” in the insulator and the “band” that crosses the chemical potential, $\omega = \mu$, in the hole-doped metal are rather similar: the low-energy band is separated from the broad valence-band background (“LHB” (lower Hubbard band) in the schematic drawings of Fig. 2) in the same way; it has similar dispersion and it has a similar intensity modulation as a function of energy. Thus, the lowest-energy metallic band appears to be effected by similar many-body physics as in the insulating regime, namely magnetic correlations connected with the (now) short-range AF order. This is not in contradiction but instead substantiated by the fact that the metallic band develops its maximum at the M-point: as pointed out above, this happens as soon as the spin-spin correlation length ξ is smaller than the length ($L=8$), a situation obtained for the filling $\langle n \rangle = 0.95$.

Furthermore, our QMC data display similarities to results derived by Kampf and Schrieffer [6]. There a phenomenological model for the spin susceptibility was used to extract the leading-order contribution to the self-energy from AF-fluctuations. The spin-spin correlation length ξ was an input parameter to the model and by varying this correlation

length the model evolved continuously from the insulating AF to the Fermi-liquid regime. For decreasing correlation length weight was transferred into the QP peak from incoherent backgrounds, which (for ξ large) developed into the upper and lower Hubbard bands (our structures “UHB” and “LHB”). This is schematically summarized in Fig. 2(b).

Another noteworthy feature of the doped, metallic situation is that the intensity change (but not the width) as a function of \vec{k} for the higher-energy background in $A(\vec{k}, \omega)$ still follows essentially the AF SDW picture with, in particular “shadow bands” resulting from the AF short-range order being clearly visible at Γ -($\omega - \mu \sim -5t$) and M-($\omega - \mu \sim +7t$) points. Even remnants can be detected of folded back “shadow bands” near the M-point for $\omega < \mu$, which in the SDW-picture have much less oscillator strength and spectral intensity than the original band (between $\Gamma \rightarrow X$) [26]. The findings confirm again to a certain extent the phenomenological work by Kampf and Schrieffer [6]. Finally, we would like to mention that an important detail of the QMC data, the rather extended flatness of the energy band near the X($\pi, 0$)-point, which is in good agreement with ARPES experiments of Dessau et al. [1] for *Bi* 2212, has previously been resolved in QMC work both for the one-band [8] and the three-band [17,27] Hubbard models. This rather extended flatness, extending like the ARPES data not only into X $\rightarrow\Gamma$, but also into the X \rightarrow M regions (as displayed in Fig. 3) is already inherent in the undoped low-energy structure near X, a fact which has recently also been found in 2-D t-J model studies by Dagotto et al. [10]. Its extension, in particular into X \rightarrow M direction, is not consistent with available one-electron band calculations [1]. It can be explained by a conventional self-energy diagrammatic analysis summing over the leading spin-fluctuation diagrams [27]. It is thus a many-body effect related to magnetic correlations consistent with the arguments given in this work.

In summary, we have studied the evolution of the 2-D Hubbard model from insulator to metal in terms of the electronic spectral weight, obtained from the maximum-entropy analytic continuation of QMC data. These results, combined with recent ARPES data, can be taken as strong indication that the QP dispersion of the high- T_c compounds, not only in the insulating limit but – particularly – in the metallic situation, has a many-body origin:

the coupling of the quasiparticles to antiferromagnetic correlations.

We would like to thank R. Laughlin, S. Maekawa, A. Muramatsu, D. Poilblanc, H. Schulz, Z.-X. Shen and, particularly, D.J. Scalapino for instructive discussions. The calculations were performed at the HLRZ Jülich and at the LRZ München.

REFERENCES

- [1] Z.-X. Shen and D.S. Dessau, Phys. Rep. (to be published); D.S. Dessau et al., Phys. Rev. Lett. **71**, 2781 (1993).
- [2] B.O. Wells, Z.-X. Shen et al., (to be published).
- [3] S.F. Gull, in *Maximum Entropy and Bayesian Methods* ed. J. Skilling, (Kluwer, Academic Publishers, 1989);
- [4] J. Skilling, in *Maximum Entropy and Bayesian Methods* ed. P.F. Fougère, (Kluwer, Academic Publishers, 1990).
- [5] J.R. Schrieffer, X.G. Wen, and S.C. Zhang, Phys. Rev. B **39**, 11663 (1989).
- [6] A.P. Kampf and J.R. Schrieffer, Phys. Rev. B **42**, 7967 (1990).
- [7] N. Bulut, D.J. Scalapino, and S.R. White, Phys. Rev. Lett. **73**, 748 (1994).
- [8] N. Bulut, D.J. Scalapino, and S.R. White, Phys. Rev. B **50**, 7215 (1994).
- [9] N. Bulut, D.J. Scalapino, and S.R. White, Phys. Rev. Lett. **72**, 705 (1994).
- [10] E. Dagotto and A. Nazarenko, M. Boninsegni, Phys. Rev. Lett. **73**, 728 (1994).
- [11] D. Poilblanc, T. Ziman, H.J. Schulz and E. Dagotto, Phys. Rev. B **47**, 14267 (1993);
D. Poilblanc et al. Phys. Rev. B **47**, 3273 (1993).
- [12] E. Dagotto, F. Ortolani and D.J. Scalapino, Phys. Rev. B **46**, 3183 (1992).
- [13] P.W. Leung, Z. Liu and E. Manousakis, M.A. Novotny, P.E. Oppenheimer, Phys. Rev. B **46**, 11779 (1992).
- [14] Y. Ohta, K. Tsutsue, W. Koshibae, T. Shimosato and S. Maekawa, Phys. Rev. B **46**, 14022 (1992).
- [15] S. Meixner, D. Poilblanc and W. Hanke, (to be published).

- [16] W. Stephan and P. Horsch, Phys. Rev. Lett. **66**, 2258 (1991).
- [17] G. Dopf, J. Wagner, P. Dieterich, A. Muramatsu, and W. Hanke, Phys. Rev. Lett. **68**, 2082 (1992).
- [18] R.N. Silver, D.S. Sivia and J.E. Gubernatis, Phys. Rev. B **41**, 2380 (1990).
- [19] S.R. White, Phys. Rev. B **44**, 4670 (1991);
- [20] S.R. White, Phys. Rev. B **46**, 5678 (1992).
- [21] W. von der Linden, Phys. Rep. **220**, 53 (1992).
- [22] R. Preuss, A. Muramatsu, W. von der Linden, P. Dieterich, F.F. Assaad, and W. Hanke, Phys. Rev. Lett. **73**, 732 (1994).
- [23] W. von der Linden, R. Preuss, and W. Hanke, to be published.
- [24] J.E. Gubernatis, M. Jarrell, R.N. Silver and D.S. Sivia, Phys. Rev. B **44**, 6011 (1991);
M. Jarrell, unpublished.
- [25] “SDW” stands here for the total integrated weight, not for the energy spread $\sim 6t$ which is significantly larger than the SDW band width.
- [26] we just received a preprint on this matter by S. Haas, A. Moreo and E. Dagotto, submitted to Phys. Rev. (1994).
- [27] R. Putz, R. Preuss, A. Muramatsu, and W. Hanke, submitted to Phys. Rev. Lett. (1994).

FIGURES

FIG. 1. Single-particle excitation for the 8×8 Hubbard model at half-filling, $U = 8t$, $\beta t = 10$: (a) The single particle spectral weight $A(\vec{k}, \omega)$ versus ω and \vec{k} ; (b) ω versus \vec{k} “bandstructure”, where sizable structure in $A(\vec{k}, \omega)$ is represented by strongly shaded areas and peaks by error bars.

FIG. 2. Schematic plot of the bandstructure: (a) the insulator and the different energy scales (see text) involved; (b) for the metallic situation.

FIG. 3. Single “bandstructure” ω versus \vec{k} for $U = 12t$, $\beta t = 3$. Again strongly shaded areas correspond to maxima of $A(\vec{k}, \omega)$.

FIG. 4. The same as Fig. 1, but now for doping $\langle n \rangle = 0.95$ and $\beta t = 3$, $U = 8t$: (a) $A(\vec{k}, \omega)$; (b) ω versus \vec{k} “bandstructure”.

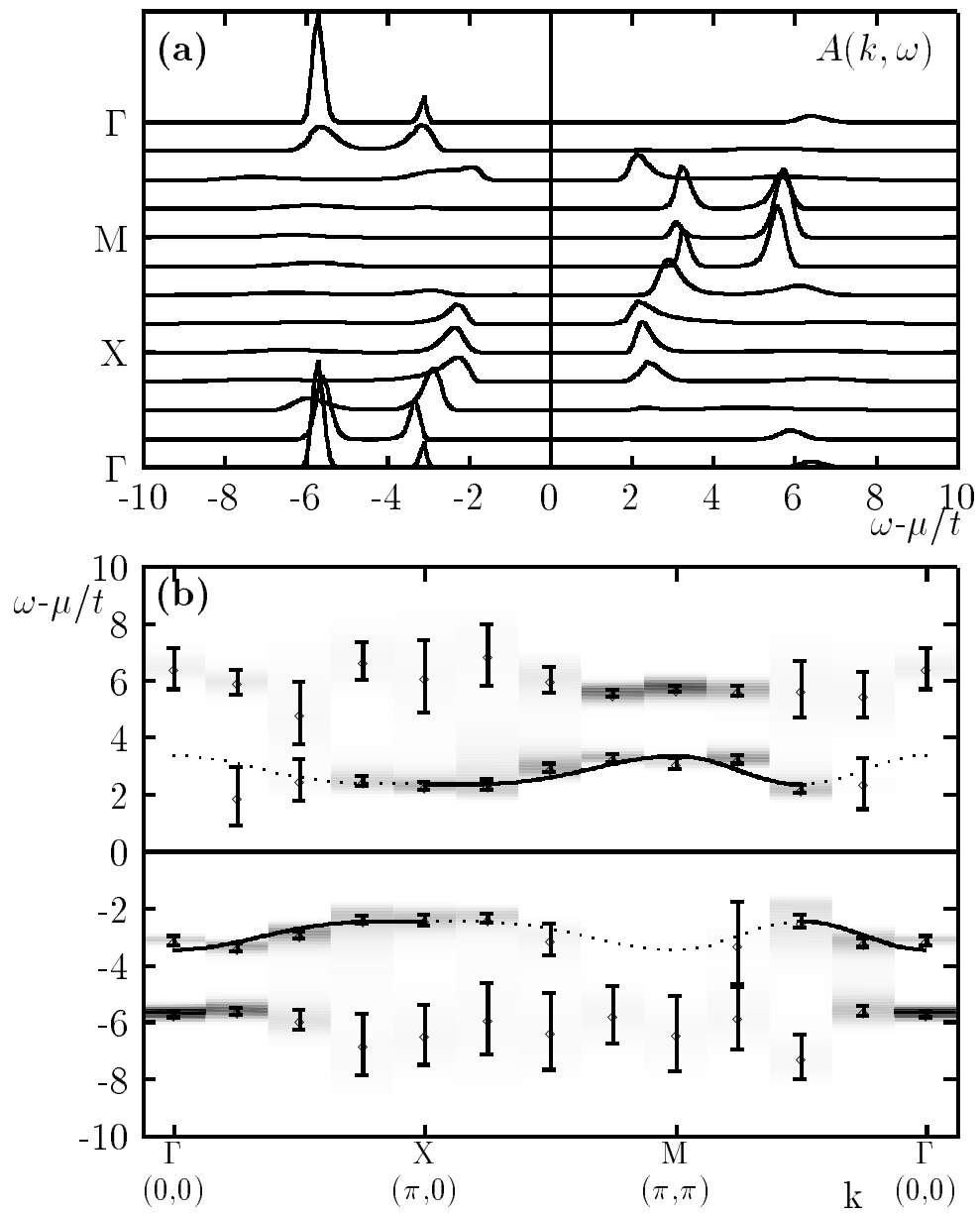


Fig. 1

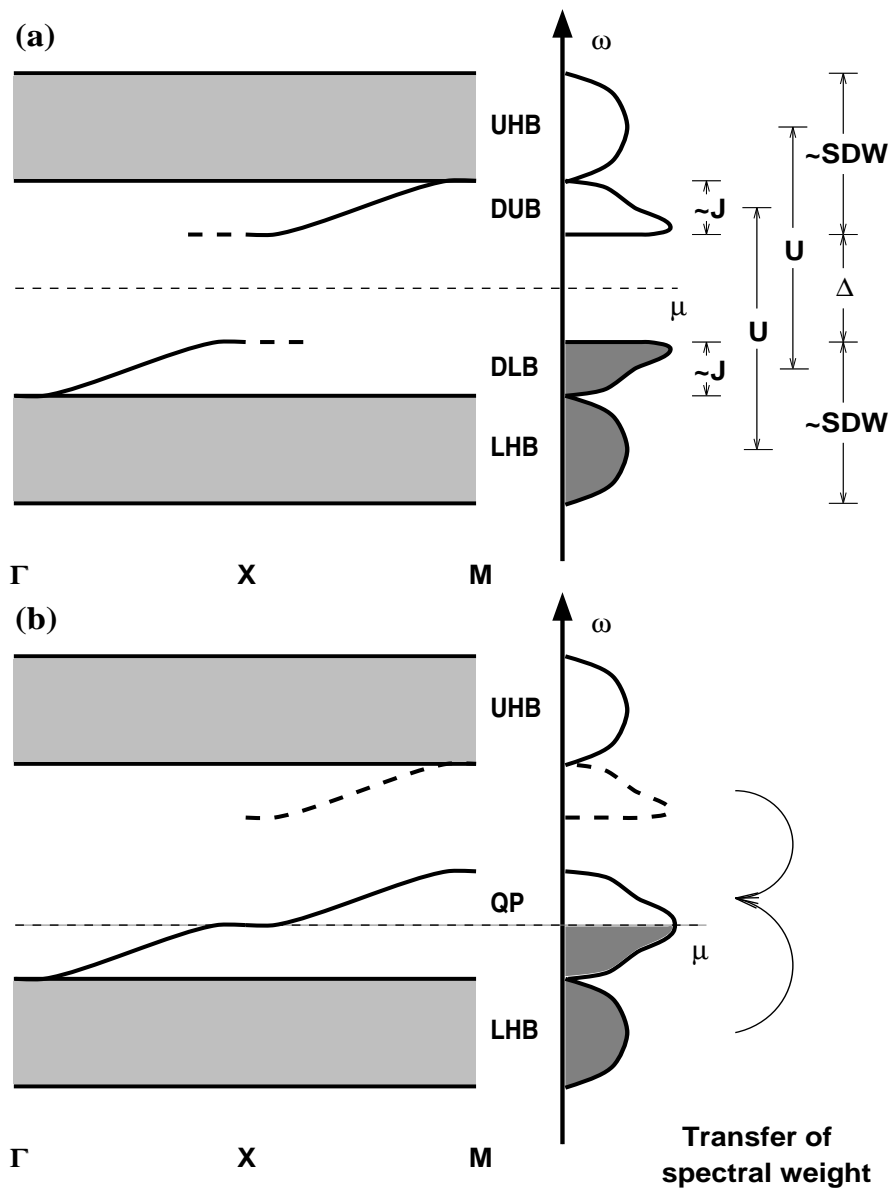


Fig. 2

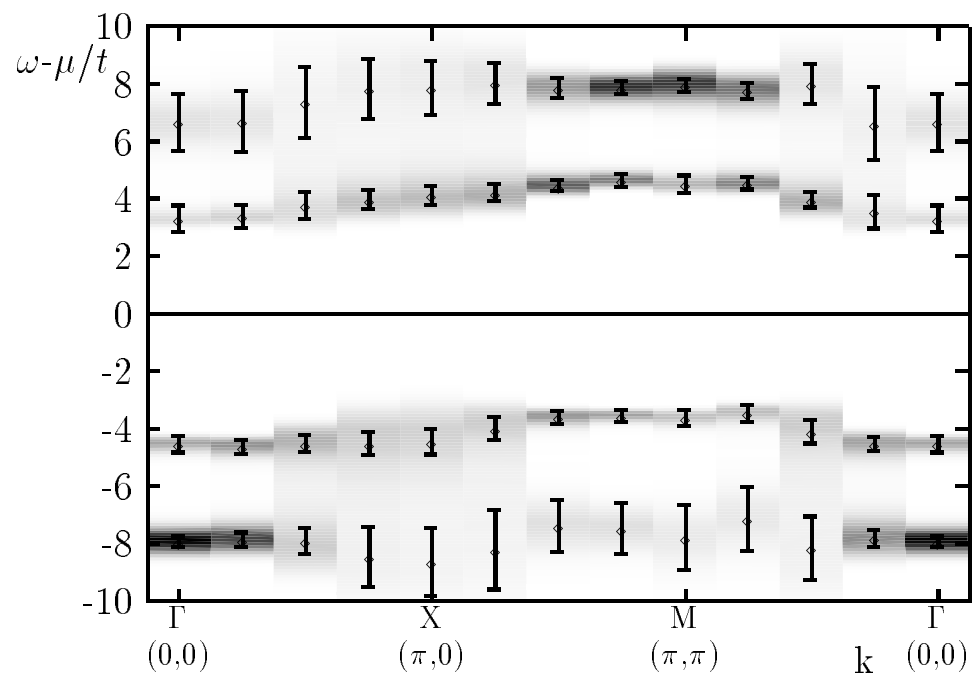


Fig. 3

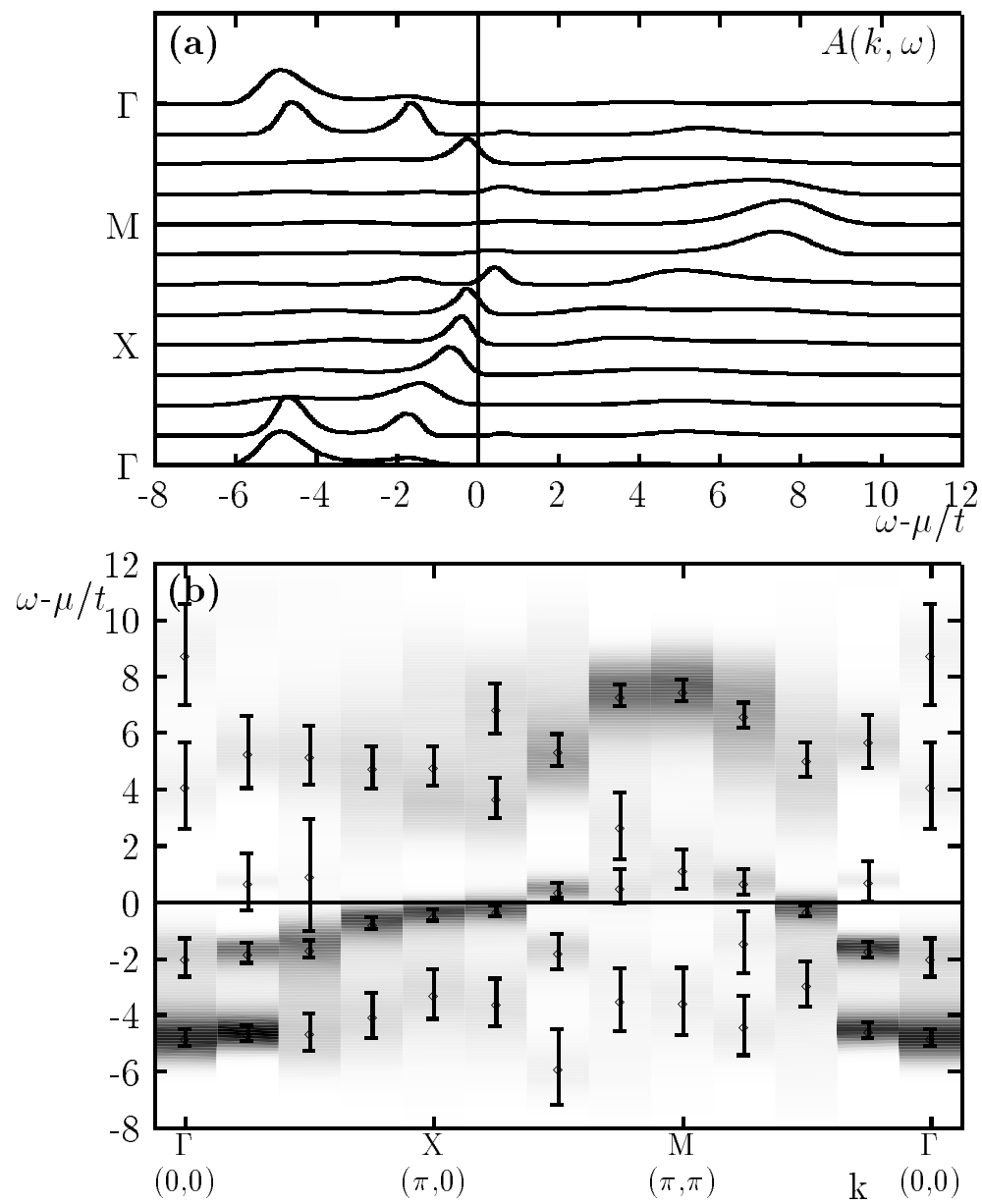


Fig. 4